

# Riddling: Chimera's dilemma

Cite as: Chaos **28**, 081105 (2018); <https://doi.org/10.1063/1.5048595>

Submitted: 16 July 2018 . Accepted: 07 August 2018 . Published Online: 23 August 2018

 V. Santos,  J. D. Szezech, A. M. Batista, K. C. Iarosz, M. S. Baptista, H. P. Ren, C. Grebogi, R. L. Viana,  I. L. Caldas, Y. L. Maistrenko, and  J. Kurths

## COLLECTIONS

 This paper was selected as Featured



[View Online](#)



[Export Citation](#)



[CrossMark](#)

## ARTICLES YOU MAY BE INTERESTED IN

**Recurrence quantification analysis for the identification of burst phase synchronisation**  
Chaos: An Interdisciplinary Journal of Nonlinear Science **28**, 085701 (2018); <https://doi.org/10.1063/1.5024324>

**Mean field phase synchronization between chimera states**

Chaos: An Interdisciplinary Journal of Nonlinear Science **28**, 091101 (2018); <https://doi.org/10.1063/1.5049750>

**Solitary states for coupled oscillators with inertia**

Chaos: An Interdisciplinary Journal of Nonlinear Science **28**, 011103 (2018); <https://doi.org/10.1063/1.5019792>



## Riddling: Chimera's dilemma

V. Santos,<sup>1</sup> J. D. Szezech, Jr.,<sup>1,2,a)</sup> A. M. Batista,<sup>1,2,3</sup> K. C. Iarosz,<sup>3,4,5</sup> M. S. Baptista,<sup>6</sup> H. P. Ren,<sup>7,8</sup> C. Grebogi,<sup>6,7</sup> R. L. Viana,<sup>9</sup> I. L. Caldas,<sup>4</sup> Y. L. Maistrenko,<sup>3,10</sup> and J. Kurths<sup>3,5</sup>

<sup>1</sup>Graduate in Science Program, State University of Ponta Grossa, Ponta Grossa, Paraná 84030-900, Brazil

<sup>2</sup>Department of Mathematics and Statistics, State University of Ponta Grossa, Ponta Grossa, Paraná 84030-900, Brazil

<sup>3</sup>Potsdam Institute for Climate Impact Research, Potsdam, Brandenburg 14473, Germany

<sup>4</sup>Institute of Physics, University of São Paulo, São Paulo, São Paulo 05508-900, Brazil

<sup>5</sup>Department of Physics, Humboldt University, Berlin, Brandenburg 12489, Germany

<sup>6</sup>Institute for Complex Systems and Mathematical Biology, SUPA, University of Aberdeen, Aberdeen AB24 3UE, Scotland, United Kingdom

<sup>7</sup>Shaanxi Key Laboratory of Complex System Control and Intelligent Information Processing, Xian University of Technology, Xi'an 710048, People's Republic of China

<sup>8</sup>Xian Technological University, Xi'an 710021, People's Republic of China

<sup>9</sup>Department of Physics, Federal University of Paraná, Curitiba, Paraná 80060-000, Brazil

<sup>10</sup>Institute of Mathematics and Centre for Medical and Biotechnical Research, National Academy of Sciences of Ukraine, Tereshchenkivska St. 3, 01030 Kyiv, Ukraine

(Received 16 July 2018; accepted 7 August 2018; published online 23 August 2018)

We investigate the basin of attraction properties and its boundaries for chimera states in a circulant network of Hénon maps. It is known that coexisting basins of attraction lead to a hysteretic behaviour in the diagrams of the density of states as a function of a varying parameter. Chimera states, for which coherent and incoherent domains occur simultaneously, emerge as a consequence of the coexistence of basin of attractions for each state. Consequently, the distribution of chimera states can remain invariant by a parameter change, and it can also suffer subtle changes when one of the basins ceases to exist. A similar phenomenon is observed when perturbations are applied in the initial conditions. By means of the uncertainty exponent, we characterise the basin boundaries between the coherent and chimera states, and between the incoherent and chimera states. This way, we show that the density of chimera states can be not only moderately sensitive but also highly sensitive to initial conditions. This chimera's dilemma is a consequence of the fractal and riddled nature of the basin boundaries.

Published by AIP Publishing. <https://doi.org/10.1063/1.5048595>

**Coupled dynamical systems have been used to describe the behaviour of real complex systems, such as power grids, neuronal networks, economics, and chemical reactions. Furthermore, these systems can exhibit various kinds of interesting nonlinear dynamics, e.g., synchronisation, chaotic oscillations, and chimera states. The chimera state is a spatiotemporal pattern characterised by the coexistence of coherent and incoherent dynamics. It has been observed in a great variety of systems, ranging from theoretical and experimental arrays of oscillators, to in phenomena such as the unihemispheric sleep of cetaceans. We study the chimera state in a circulant network of Hénon maps, seeking to determine how the density of states in the network depends on the system parameters and the initial conditions. We have found that, as expected, the density of states might be invariant to parameter alterations, but it might also tip when a basin of attraction ceases to exist. When the basin boundary of the chimera states is fractal, the densities of the states will depend moderately on the perturbations in the initial conditions, and they may even remain invariant to specific perturbations. However, when the basin boundary is riddled, even arbitrarily small perturbations to the initial conditions can replace the chimera state to an incoherent state. The existence of basin boundary in**

**a network that presents chimera states is a chimera's dilemma.**

### I. INTRODUCTION

Chimera state, in reference to the Greek mythological creature, is a spatiotemporal pattern observed in coupled dynamical systems that was first reported by Kuramoto and Battogtokh in 2002.<sup>1</sup> This pattern is characterised by the coexistence of coherent and incoherent behaviours.<sup>2–6</sup> It has been identified in paradigmatic network models,<sup>7,8</sup> such as the Kuramoto model,<sup>9,10</sup> networks of Hindmarsh-Rose neurons,<sup>11</sup> and coupled van der Pol-Duffing oscillators.<sup>12</sup> Chimera states have also been found in experimental settings.<sup>13</sup> Martens *et al.*<sup>14</sup> showed them in a mechanical experiment composed of coupled metronomes. Kapitaniak *et al.*<sup>15</sup> demonstrated the formation of chimera in Huygens's clocks realised by metronomes. Coupled electronic oscillators can exhibit chimera with quiescent and synchronous domains.<sup>16</sup>

Basins of attraction for chimera states were analysed by Martens *et al.*<sup>17</sup> They considered two coupled populations of Kuramoto-Sakaguchi. The chimera states have a coexisting asynchronous and synchronous population, where their basins of attraction show a complex twist structure. Rakshit *et al.*<sup>18</sup> identified and quantified incoherent, coherent, and chimera

<sup>a)</sup>Electronic mail: jdsjunior@uepg.br

states in coupled time-delayed Mackey-Glass oscillators by means of basin stability analysis. The coexisting basins were found to be roughly robust to the coupling strength and coupling radius alterations in certain network configurations, i.e., the density of the chimera states could be preserved by the coupling strength and the coupling radius alterations for those configurations. Our interest is to understand this stability of the density of the states in terms of initial conditions. To this goal, we analyse a circulant network composed of Hénon maps and characterise its basin boundaries for chimera states.

The Hénon map was proposed as a simplified model to study the dynamics of the Lorenz model.<sup>19</sup> Networks of coupled Hénon maps have been considered in studies about periodic orbits,<sup>20</sup> chaotic dynamics of spatially extended systems,<sup>21</sup> and unstable dimension variability structure.<sup>22</sup> Semenova *et al.* have recently found chimera states in ensembles of non-locally coupled Hénon maps.<sup>23</sup> They also explored the effects of noise perturbations on the network.

In this work, we calculate the strength of incoherence to identify incoherent, coherent, and chimera states. Clearly, each network state (coherent or incoherent) has its own basin of attraction. Parameter changes modify the Lebesgue measure of the basins, which in extreme situations can cease to exist, leaving a network whose nodes will be in either the coherent or incoherent states. Our main interest, however, is to understand how perturbations in the initial conditions change the density of these states in the network. To this goal, we study the property of the basins of attraction's boundaries. We find that whereas the basin boundary between the incoherent and chimera states is typically riddled, the basin boundary between the chimera and the coherent state is typically fractal. Thus, small alterations in the initial conditions can always change the density of the states. However, arbitrarily small perturbations in the initial conditions can shift a chimera state to an incoherent one.

Riddled basin is a basin of attraction (of an attractor) such that every point of it has pieces of another attractor's basin arbitrarily nearby.<sup>24–26</sup> A riddled basin of attraction has the same fractal dimension of its boundary. Heagy *et al.*<sup>27</sup> reported experimental and numerical evidence of riddled basins in coupled chaotic systems. They studied chaos synchronisation in coupled chaotic oscillator circuits. Woltering and Markus<sup>28</sup> identified the existence of riddled basin in a model for the Belousov-Zhabotinsky reaction.

This paper is organised as follows: Section II introduces the network of coupled maps. In Sec. III, we present the basin of attraction for chimera states and our results for the basin boundaries. In the last section, we draw our conclusions.

## II. NETWORK MODEL

Networks of coupled maps have been used to study the extended dynamical system.<sup>29</sup> We consider a network composed of  $N$  coupled Hénon maps written as

$$\mathbf{x}_{t+1}^{(i)} = \mathbf{F}(\mathbf{x}_t^{(i)}) + \frac{\sigma \mathbf{E}}{2rN} \sum_{j=i-rN}^{i+rN} [\mathbf{F}(\mathbf{x}_t^{(j)}) - \mathbf{F}(\mathbf{x}_t^{(i)})], \quad (1)$$

where  $i = 1, \dots, N$ ,  $t$  is the discrete time,  $\mathbf{F}(\mathbf{x}) = [1 - \alpha x^2 + y, \beta x]^T$  is the two-dimensional Hénon map,  $\sigma$  and  $r$  are the coupling intensity and coupling radius, respectively, and

$$\mathbf{E} = \begin{pmatrix} 1 & 0 \\ 0 & 0 \end{pmatrix}, \quad (2)$$

specifies which variables of the Hénon map are coupled here, namely,  $x$ . This system was previously studied by Semenova *et al.*<sup>30</sup> for the parameter set  $(\alpha, \beta) = (1.4, 0.3)$  focusing on the parameter space  $\sigma \times r$ . In our network, we use  $(\alpha, \beta) = (1.44, 0.164)$ , because the Hénon map exhibits a period-5 attractor for these parameters. We consider a circulant network of Hénon maps. Figure 1(a) shows the spatiotemporal plot obtained from Eq. (1) for  $\sigma = 0.30$  and  $r = 0.30$ , where the colour bar represents the variable  $x^{(i)}$ . We find two coherent and one incoherent (small region around  $i = 250$ ) domains, as shown in Fig. 1(b). The discontinuities in  $x^{(87)}$  and  $x^{(412)}$  are due to the splitting of the spatial profile into two branches, while the interval region from approximately  $x^{(220)}$  to  $x^{(280)}$  displays spatial incoherence (irregular spatial pattern). A chimera state of the form as in Figs. 1(a) and 1(b) was first reported by Omelchenko *et al.*<sup>31</sup>

Aiming to characterise coherent and incoherent states, we use a quantitative measure proposed by Gopal *et al.*<sup>32</sup> To do that, first, we calculate  $s_m = \Theta[\delta - \chi(m)]$ , where  $\Theta$  is the Heaviside step function and  $\delta$  is a predetermined threshold. The local standard deviation  $\chi^{(l)}(m)$  is given by

$$\chi^{(l)}(m) = \sqrt{\left\langle \frac{1}{n} \sum_{j=n(m-1)+1}^{nm} [z^{(l,j)} - \langle z^{(l)} \rangle]^2 \right\rangle_t}, \quad (3)$$

where  $n = N/M$ ,  $m = 1, 2, \dots, M$ , and  $\mathbf{z}_t^{(i)} = \mathbf{x}_t^{(i)} - \mathbf{x}_t^{(i+1)}$  with  $\mathbf{z}^{(i)} = [z^{(1,i)}, z^{(2,i)}, \dots, z^{(d,i)}]^T \in \mathbb{R}^d$ , and  $d$  is the dimension of the dynamical system. In these new variables, two neighbouring oscillators describing a node of the network  $i$  and  $i+1$  are oscillating coherently if  $\mathbf{z}^{(i)} \approx 0$  and incoherently otherwise.  $\langle z^{(l)} \rangle = \frac{1}{n} \sum_{j=n(m-1)+1}^{nm} z_t^{(l,j)}$  is the average of  $z_t^{(l)}$  over the partition  $m$  for a fixed time, and  $\langle \dots \rangle_t$  is the time

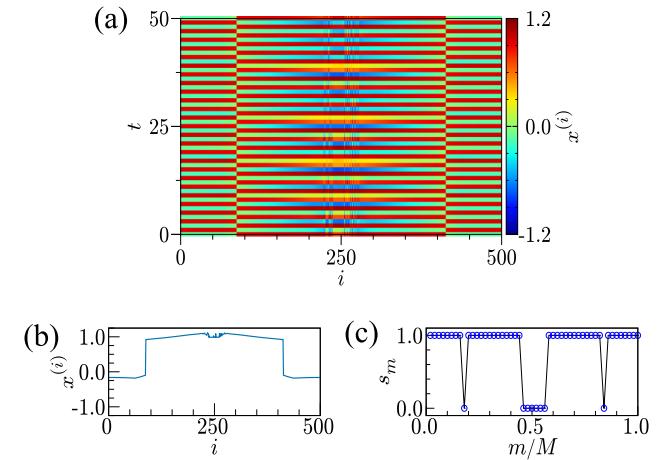


FIG. 1. (a) Space-time plot of the dynamics of the network Eq. (1) after the transient time, where the colour bar gives the value of the  $x$  variable of each map in the network. In (b) and (c), we plot the snapshot and its  $s_m$  spectrum, respectively, for  $t = 26$  of (a). We consider  $\alpha = 1.44$ ,  $\beta = 0.164$ ,  $\sigma = 0.30$ , and  $r = 0.30$ .

average. We set  $\delta = 1\%$  of  $|x^{(l,\max)} - x^{(l,\min)}|$ , and the network size  $N = 500$ . Figure 1(c) shows  $s_m$  for the network separated into  $M = 50$  partitions. By means of  $s_m$  versus  $m/M$ , we can clearly identify the coherent and incoherent regions.

Gopal *et al.*<sup>32</sup> developed the measure *strength of incoherence* (SI) to characterise the spatial dynamics of nonlinear coupled networks. It is able to identify coherent and incoherent states, as well as chimera states.<sup>18,32</sup> The SI is given by

$$SI = 1 - \frac{\sum_{m=1}^M s_m}{M}. \quad (4)$$

If  $\chi^{(l)}(m) > \delta$ , some of the oscillators in the  $m$ -th partition are incoherent and  $s_m = 0$ . When  $N \rightarrow \infty$ ,  $SI \rightarrow 1$  ( $s_m = 0, \forall m$ ) for incoherent states,  $SI \rightarrow 0$  for coherent and cluster states, and  $0 < SI < 1$  for chimera states. In Fig. 2(a), we plot SI versus the coupling strength  $\sigma$  for 400 different initial conditions of the system (1). We consider  $(x_0^{(i)}, y_0^{(i)}) = (0, 0)$  for  $i = 2, \dots, N$ , and  $(x_0^{(1)}, y_0^{(1)})$  is homogeneously distributed in the interval  $[-3, 3] \times [-3, 3]$ . The state variable is iterated 10 500 times, with the first 9000 being discarded as transient state, and the last 1500 are included to calculate SI. The accuracy of our results is not improved by doubling the size of the dataset. The long transient is considered to avoid treating transient chimera states as an asymptotic state.

Figure 2(a) shows the coexistence of multiple states with different values of SI for the same  $\sigma$  in the interval  $[0.08, 0.44]$ . This hysteresis course reflects that the basin of attraction for the coherent and the incoherent states coexists. For smaller values of the coupling strength, there is only the incoherent state (characterised by the red curve for  $SI = 1$ ), and its large basin of attraction occupies a large domain of initial conditions considered (excluding the infinity basin). About  $\sigma \approx 0.08$ , the coexistence of three basins of attractions causes the network to behave either in the coherent state (smaller SI values), in the incoherent state (larger SI values), or in the chimera (intermediate SI values). Appropriately chosen initial conditions may lead a network whose  $\sigma$  is being altered to have states characterised by the red curve until  $\sigma = 0.5$ . For intermediate  $\sigma$  values, the network is characterised by coherent and chimera states with lower SI values. At  $\sigma = 0.5$ , there is only the basin of attraction for the coherent states. For appropriately chosen initial conditions, as  $\sigma$  is varied from 0.5 to zero, the network might present a distinct route from coherence to incoherence (characterised by the SI for the black curve). This means that the network has a hysteresis behaviour for its states, typical to happen in networks that present chimera. Figure 2(b) exhibits the single node basin stability (BS) as a function of  $\sigma$  for incoherent (black), chimera (red), coherent (gray), and divergent (white) states. BS is associated with the volume of the basin of attraction.<sup>33–35</sup> In Figs. 2(c)–2(h), we plot snapshots of the dynamic behaviour for  $\sigma = 0.24$ . Changing the initial conditions of only one map of the network, we observe (c) synchronised period-5 dynamics corresponding to  $SI = 0.00$ , (d) period-2 cluster state in which  $SI = 0.04$ , (e) to (g) chimera states for different sizes of incoherent states with  $SI = 0.24$ ,  $SI = 0.42$ , and  $SI = 0.76$ , respectively, and (h) incoherent state for which  $SI = 1.00$ .

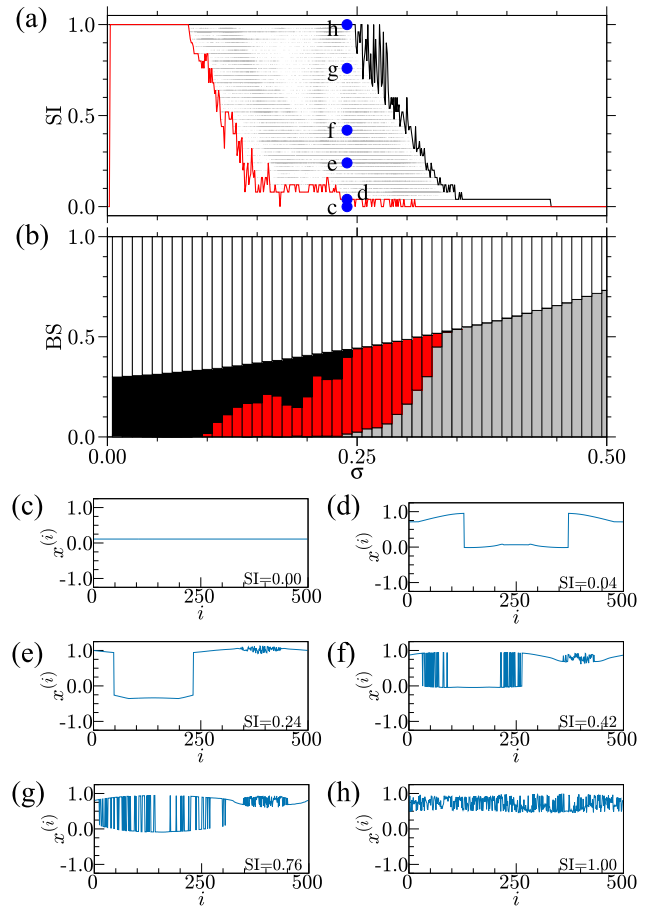


FIG. 2. (a) SI versus  $\sigma$  for 400 different initial conditions. The red (black) line outlines the minimum (maximum) value of SI. (b) BS versus  $\sigma$  for incoherent (black), chimera (red), coherent (gray), and divergent (white) states. From (c) to (h), we plot some coexistent states for  $\sigma = 0.24$ . We consider  $\alpha = 1.44$ ,  $\beta = 0.164$ , and  $r = 0.30$ .

### III. BASIN OF ATTRACTION FOR CHIMERA STATES

In our network, for some values of  $\sigma$ , a great variety of dynamical states can be found by only changing the initial conditions. With this in mind, we investigate this phenomenon by means of the basin of attraction. To do that, we construct a

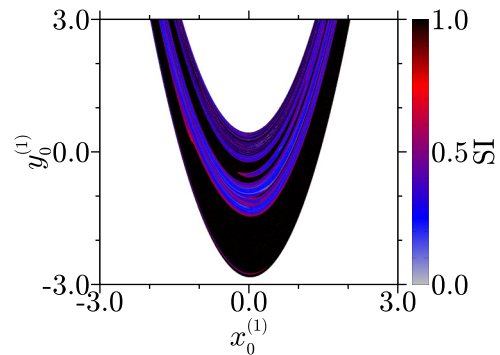


FIG. 3. Basin of attraction of only 1 Hénon map in the network with  $\sigma = 0.18$ ,  $\alpha = 1.44$ ,  $\beta = 0.164$ , and  $r = 0.30$ , where the colour bar represents the SI values. The black points correspond to incoherent states, the grey points denote the synchronised cluster states, from blue to red points represent the chimera states. The initial conditions in the white region diverge to infinity.

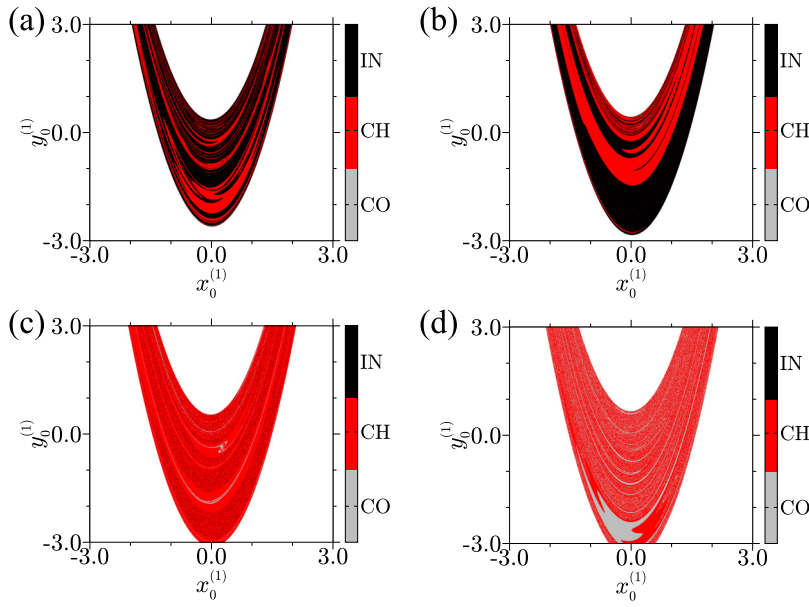


FIG. 4. Basins of attraction of the network of coupled Hénon maps for coherent (CO), chimera (CH), and incoherent (IN) states. We consider  $\sigma$  equal to (a) 0.12, (b) 0.18, (c) 0.24, and (d) 0.30.

grid and vary the initial values of the variables of one map of the network, while the others are kept equal to 0.

In Fig. 3, we plot the basin of attraction for  $\sigma = 0.18$  with the SI values being represented by a colour scale. It displays the same overall shape of the basin of one individual Hénon map. From Fig. 3, it can be noted that the density of each state varies depending on the region where we sort the initial conditions; also, in some regions, the boundaries between the basins may be very complex.

In order to analyse the basin boundaries, we define  $SI \leq 0.04$  as coherent state,  $SI \geq 0.90$  as incoherent state, and intermediate values as chimera states. Applying these thresholds, we plot the basin for  $\sigma = 0.12, 0.18, 0.24$ , and  $0.30$ , as shown in Fig. 4, with gray standing for coherent (CO), red for chimera (CH), and black for incoherent (IN) states. When  $\sigma$  is small, there is a predominance of incoherent and chimera states in the basins. Increasing the value of  $\sigma$ , we find a

decrease in the size of the basin for incoherent states and an increase in that for coherent states. The basins are arranged in a complicated way with some regions exhibiting an apparent fractal structure. It was demonstrated that fractality in the basin boundary can strongly affect the predictability of final states in dynamical systems.<sup>36</sup>

The characterisation of basin boundaries can be made using the initial condition uncertainty fraction, as introduced by McDonald *et al.*<sup>36</sup> The method consists of calculating the final state of a number  $N_0$  of random initial conditions in a region of the basin. If the final state from a point in the center of a neighbourhood of radius  $\varepsilon$  is different from at least one of its neighbours, then such an initial condition is  $\varepsilon$ -uncertain. The fraction of uncertain points  $f(\varepsilon)$  as a function of  $\varepsilon$ , for small  $\varepsilon$ , is expected to scale according to  $f(\varepsilon) \sim \varepsilon^\gamma$ , where  $\gamma$  is the uncertainty exponent.<sup>37,38</sup> The  $\gamma$  is related to the boundary of the sets being considered (here they are the basin of

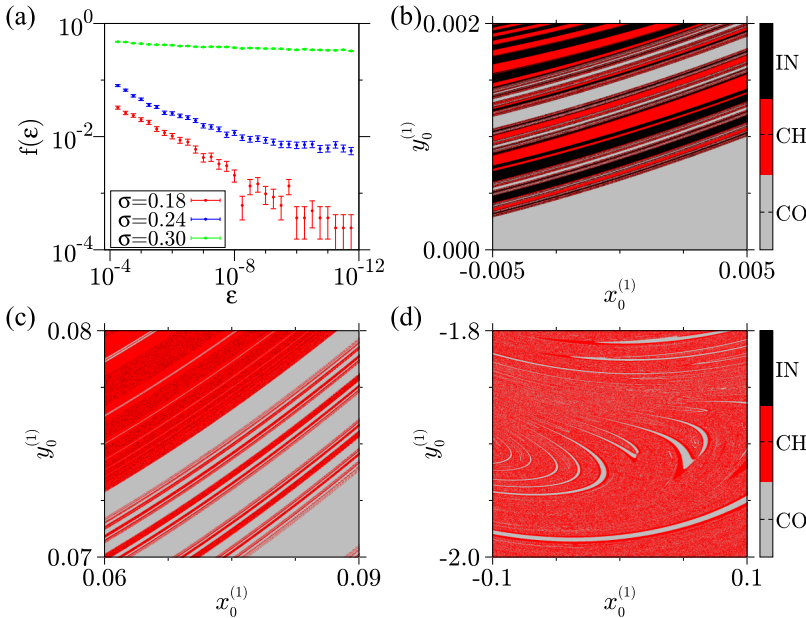


FIG. 5. (a) Uncertainty fraction  $f(\varepsilon)$  versus the uncertainty radius  $\varepsilon$  for the boundary between the chimera and the coherent basins. Magnification of the basin of attraction for (b)  $\sigma = 0.18$ , (c)  $\sigma = 0.24$ , and (d)  $\sigma = 0.30$ .

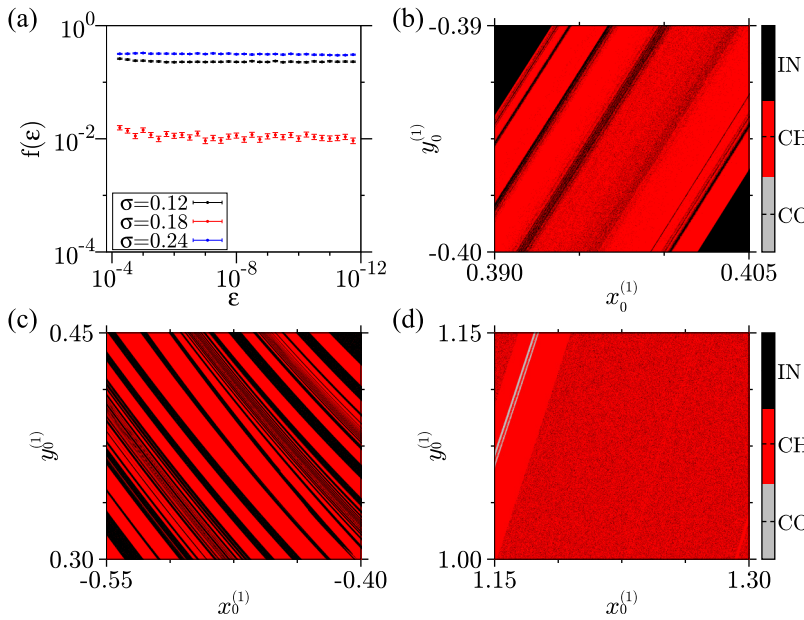


FIG. 6. (a) Uncertainty fraction  $f(\varepsilon)$  versus the uncertainty radius  $\varepsilon$  for the boundary between the incoherent and chimera state basins. Magnification of the basin of attraction for (b)  $\sigma = 0.12$ , (c)  $\sigma = 0.18$ , and (d)  $\sigma = 0.24$ .

attractions) by  $d = D - \gamma$ , where  $d$  is the dimension of the basin boundary and  $D = 2$  is the phase space dimension of the boxes used to calculate  $\gamma$ .

Firstly, we calculate  $f(\varepsilon)$  for the boundary between the chimera and coherent state basins, as shown in Fig. 5(a). Figures 5(b)–5(d) show magnifications of Figs. 4(b)–4(d) that allow one to see the complexity of the boundaries. We use the interval of the magnifications to estimate  $f(\varepsilon)$  versus  $\varepsilon$ . For  $\sigma = 0.12$ , the basin of the coherent states is very small; therefore, it can be neglected. From the fitting of the points of Fig. 5(a), we obtain  $\gamma = 0.30$  (red dots),  $\gamma = 0.15$  (blue dots), and  $\gamma = 0.02$  (green dots) for  $\sigma = 0.18, 0.24$ , and 0.30, respectively. As a result, the boundaries between the chimera and coherent state basins are fractal. A positive and constant uncertainty coefficient means that the closer you are to an initial condition, the more likely you are of generating the same final state of the one generated by that initial condition. The further you go, the more likely you are changing states by a perturbation in the initial condition. One consequence of this observation is that there is a positive probability of a network in the coherent state to transit to the chimera state if an initial condition used is perturbed. Since a coherent state can be set by placing all the initial conditions as equal, it is reasonable to expect that by changing the initial condition of one node of the network (as we have actually done), one can reach the chimera state. Another consequence is that the chimera state can be replaced by the coherent state by a perturbation in the initial conditions as well. This is a consequence of the fact that the uncertainty coefficient is positive, and therefore, no matter the precision one alters the initial conditions, there is always a positive probability for the state to change. However, since the basin has a fractal boundary, there exist particular directions to change the initial conditions such that the chimera can be preserved. This direction is the one associated with the direction where the dimension is not fractal. All in all, the point is that the chimera state in the observed network can be found, preserved, or altered by design, if one wishes so, as long as the initial conditions are set about the boundary of the

coherent and the chimera states. The same does not happen with respect to the incoherent state.

Secondly, we compute  $f(\varepsilon)$  for the boundary between the chimera and incoherent state basins, as shown in Fig. 6(a). In Figs. 6(b)–6(d), we plot magnifications of Figs. 4(a)–4(c) emphasising the boundary between incoherent and chimera state basins. The incoherent state basin has a very small size for  $\sigma = 0.30$ . Our results show that  $f(\varepsilon)$  remains approximately constant for different  $\sigma$  values, and as a consequence  $\gamma \approx 0$ , indicating the existence of a riddled basin. A zero uncertainty coefficient means that the probability of finding an uncertain box, regardless of the resolution of the boxes used (with sides  $\varepsilon$ ), is constant. No matter how small or large is the perturbation applied to an initial condition, the change that the system will take place is the same. This is so because of the riddled basin for which the dimension of the boundary of the basins of attraction is the dimension of the basin itself. Thus, in such a situation, a special direction does not exist for initial conditions to be perturbed in order to maintain the incoherent state. In contrast to what was reported before, the preservation or alteration of the chimera state by a modification in the initial conditions cannot be done by design but only in a statistical sense. Therefore, these facts lead us to conclude that the existence of a riddled basin boundary in a network that presents chimera is a chimera's dilemma. It makes the state to be fragile by arbitrarily small changes in the initial conditions.

#### IV. CONCLUSIONS

We have analysed a network of circulant coupled Hénon maps. This network is a discrete time dynamical system that exhibits coherent and incoherent behaviours. We consider parameter values where coherent and incoherent domains, named chimera state, coexist.

The chimera state coexists with the other two states, namely, the coherent and the incoherent states. All these states have their attraction basin boundaries. It is known that due to this coexistence, the network may present hysteretic

behaviour as parameters are increased or decreased. The hysteresis character of the chimera and its coexisting states, where attractors and their basins can disappear or bifurcate, can potentially provide clarifications about the emergence of tipping points in nature.<sup>39</sup> Typically, tipping points are explained in terms of lower dimensional systems with the coexistence of states such as equilibrium points or limit cycles. The chimera state could itself be considered as a possible reason for tipping points emerging in large dimensional networked systems. Our main interest in this work is to study properties of the boundary between two of these states, the incoherent and chimera, and the chimera and coherent states. Through the uncertainty exponent, we uncover that the basin boundaries between the coherent and chimera states are fractal, while the basin boundary of incoherent and chimera states are riddled. Consequently, the first case is more robust to perturbations in the initial conditions than the second one. Whereas one is likely to obtain a chimera state by a perturbation of initial conditions leading to the coherent state (which can be set by having all nodes with the same or roughly the same initial condition), it is unlikely to appear a chimera state by a perturbation of initial conditions leading to the incoherent state.

## ACKNOWLEDGMENTS

We wish to acknowledge the support from São Paulo Research Foundation (FAPESP) under Grant Nos. 2011/19296-1, 2015/05186-0, 2015/07311-7, 2015/50122-0, and 2017/20920-8, Conselho Nacional de Desenvolvimento Científico e Tecnológico (CNPq), and Coordenação de Aperfeiçoamento de Pessoal de Nível Superior (CAPES).

<sup>1</sup>Y. Kuramoto and D. Battogtokh, “Coexistence of coherence and incoherence in nonlocally coupled phase oscillators,” *Nonlinear Phenom. Complex Syst.* **5**, 380 (2002).

<sup>2</sup>K. Umberger, C. Grebogi, E. Ott, and B. Afeyan, “Spatio-temporal dynamics in a dispersively coupled chain of nonlinear oscillators,” *Phys. Rev. A* **39**, 4835 (1989).

<sup>3</sup>D. M. Abrams and S. H. Strogatz, “Chimera states for coupled oscillators,” *Phys. Rev. Lett.* **93**, 174102 (2004).

<sup>4</sup>D. M. Abrams, R. Mirolo, S. H. Strogatz, and D. A. Wiley, “Solvable model for chimera states of coupled oscillators,” *Phys. Rev. Lett.* **101**, 084103 (2008).

<sup>5</sup>I. Omelchenko, Y. Maistrenko, P. Hövel, and E. Schöll, “Loss of coherence in dynamical networks: Spatial chaos and chimera states,” *Phys. Rev. Lett.* **106**, 234102 (2011).

<sup>6</sup>D. Dudkowski, Y. Maistrenko, and T. Kapitaniak, “Different types of chimera states: An interplay between spatial and dynamical chaos,” *Phys. Rev. E* **90**, 032920 (2014).

<sup>7</sup>O. E. Omel’chenko, Y. L. Maistrenko, and P. A. Tass, “Chimera states: The natural link between coherence and incoherence,” *Phys. Rev. Lett.* **100**, 044105 (2008).

<sup>8</sup>R. G. Andrzejak, G. Ruzzene, and I. Malvestio, “Generalized synchronization between chimera states,” *Chaos* **27**, 053114 (2017).

<sup>9</sup>M. S. Santos, J. D. Szezech Jr, A. M. Batista, I. L. Caldas, R. L. Viana, and S. R. Lopes, “Recurrence quantification analysis of chimera states,” *Phys. Lett. A* **379**, 2188 (2015).

<sup>10</sup>N. Yao, Z.-G. Huang, C. Grebogi, and Y.-C. Lai, “Emergence of multicluster chimera states,” *Sci. Rep.* **5**, 12988 (2015).

<sup>11</sup>M. S. Santos, J. D. Szezech, F. S. Borges, K. C. Iarosz, I. L. Caldas, A. M. Batista, R. L. Viana, and J. Kurths, “Chimera-like states in a neuronal network model of the cat brain,” *Chaos Solitons Fractals* **101**, 86 (2017).

<sup>12</sup>D. Dudkowski, Y. Maistrenko, and T. Kapitaniak, “Occurrence and stability of chimera states in coupled externally excited oscillators,” *Chaos* **26**, 116306 (2016).

<sup>13</sup>M. R. Tinsley, S. Nkomo, and K. Showalter, “Chimera and phase-cluster states in populations of coupled chemical oscillators,” *Nat. Phys.* **8**, 662 (2012).

<sup>14</sup>E. A. Martens, S. Thutupalli, A. Fourrière, and O. Hallatschek, “Chimera states in mechanical oscillator networks,” *Proc. Natl. Acad. Sci.* **110**, 10563 (2013).

<sup>15</sup>T. Kapitaniak, P. Kuzma, J. Wojewoda, K. Czolczynski, and Y. Maistrenko, “Imperfect chimera states for coupled pendula,” *Sci. Rep.* **4**, 6379 (2014).

<sup>16</sup>L. B. Gambuzza, A. Buscarino, S. Chessari, L. Fortuna, R. Meucci, and M. Frasca, “Experimental investigation of chimera states with quiescent and synchronous domains in coupled electronic oscillators,” *Phys. Rev. E* **90**, 032905 (2014).

<sup>17</sup>E. A. Martens, M. J. Panaggio, and D. M. Abrams, “Basins of attraction for chimera states,” *New J. Phys.* **18**, 022002 (2016).

<sup>18</sup>S. Rakshit, B. K. Bera, M. Perc, and D. Ghosh, “Basin stability for chimera states,” *Sci. Rep.* **7**, 2412 (2017).

<sup>19</sup>M. Hénon, “Numerical study of quadratic area-preserving mappings,” *Quart. Appl. Math.* **27**, 291 (1969).

<sup>20</sup>A. Politi and A. Torcini, “Periodic orbits in coupled Hénon maps: Lyapunov and multifractal analysis,” *Chaos* **2**, 293 (1992).

<sup>21</sup>V. Astakhov, A. Shabunin, W. Uhm, S. Kim, “Multistability formation, synchronization loss in coupled Hénon maps: Two sides of the single bifurcational mechanism,” *Phys. Rev. E* **63**, 056212 (2001).

<sup>22</sup>V. Santos, J. D. Szezech Jr, M. S. Baptista, A. M. Batista, and I. L. Caldas, “Unstable dimension variability structure in the parameter space of coupled Hénon maps,” *Appl. Math. Comput.* **286**, 23 (2016).

<sup>23</sup>N. I. Semenova, G. I. Strelkova, V. S. Anishchenko, and A. Zakharova, “Temporal intermittency and the lifetime of chimera states in ensembles of nonlocally coupled chaotic oscillators,” *Chaos* **27**, 061102 (2017).

<sup>24</sup>J. C. Alexander, J. A. Yorke, Z. You, and I. Kan, “Riddled basins,” *Int. J. Bifurcat. Chaos* **2**, 795 (1992).

<sup>25</sup>E. Ott, J. C. Sommerer, J. C. Alexander, I. Kan, and J. A. Yorke, “Scaling behavior of chaotic systems with riddled basins,” *Phys. Rev. Lett.* **71**, 4134 (1993).

<sup>26</sup>P. Ashwin, J. Buescu, and I. Stewart, “Bubbling of attractors and synchronization of chaotic oscillators,” *Phys. Lett. A* **193**, 126 (1994).

<sup>27</sup>J. F. Heagy, T. L. Carroll, and L. M. Pecora, “Experimental and numerical evidence for riddled basins in coupled chaotic systems,” *Phys. Rev. Lett.* **73**, 3528 (1994).

<sup>28</sup>M. Woltering and M. Markus, “Riddled basins in a model for the Belousov-Zhabotinsky reaction,” *Chem. Phys. Lett.* **321**, 473 (2000).

<sup>29</sup>K. Kaneko, “Overview of coupled map lattices,” *Chaos* **2**, 279 (1992).

<sup>30</sup>N. Semenova, A. Zakharova, E. Schöll, and V. Anishchenko, “Does hyperbolicity impede emergence of chimera states in networks of nonlocally coupled chaotic oscillators?,” *Europhys. Lett.* **112**, 40002 (2015).

<sup>31</sup>I. Omelchenko, B. Riemenschneider, P. Hövel, Y. Maistrenko, and E. Schöll, “Transition from spatial coherence to incoherence in coupled chaotic systems,” *Phys. Rev. E* **85**, 026212 (2012).

<sup>32</sup>R. Gopal, V. K. Chandrasekar, A. Venkatesan, and M. Lakshman, “Observation and characterization of chimera states in coupled dynamical systems with nonlocal coupling,” *Phys. Rev. E* **89**, 052914 (2014).

<sup>33</sup>P. J. Menck, J. Heitzig, N. Marwan, and J. Kurths, “How basin stability complements the linear-stability paradigm,” *Nat. Phys.* **9**, 89 (2013).

<sup>34</sup>P. J. Menck, J. Heitzig, J. Kurths, and H. J. Schellnhuber, “How dead ends undermine power grid stability,” *Nat. Commun.* **5**, 3969 (2014).

<sup>35</sup>P. Schultz, P. J. Menck, J. Heitzig, and J. Kurths, “Potentials and limits to basin stability estimation,” *New J. Phys.* **19**, 023005 (2017).

<sup>36</sup>S. W. McDonald, C. Grebogi, E. Ott, and J. A. Yorke, “Fractal basin boundaries,” *Physica D* **17**, 125 (1985).

<sup>37</sup>C. Grebogi, E. Kostelich, E. Ott, J. A. Yorke, “Multi-dimensioned intertwined basin boundaries: Basin structure of the kicked double rotor,” *Physica D* **25**, 347 (1987).

<sup>38</sup>J. Aguirre, R. L. Viana, and M. A. F. Sanjuán, “Fractal structures in nonlinear dynamics,” *Rev. Mod. Phys.* **81**, 333 (2009).

<sup>39</sup>E. S. Medeiros, I. L. Caldas, M. S. Baptista, and U. Feudel, “Trapping phenomenon attenuates the consequence of tipping points for limit cycles,” *Sci. Rep.* **7**, 42351 (2017).